Matthews, John A., Owen, Geraint, Winkler, Stefan, Vater, Amber E., Wilson, Peter, Mourne, Richard W. and Hill, Jennifer ORCID logoORCID: https://orcid.org/0000-0002-0682-783X (2016) A rock-surface microweathering index from Schmidt hammer R-values and its preliminary application to some common rock types in southern Norway. Catena, 143. pp. 35-44. doi:10.1016/j.catena.2016.03.018

A rock-surface microweathering index from Schmidt hammer R-values and its preliminary application to some common rock types in southern Norway

John A. Matthews[1], Geraint Owen[1], Stefan Winkler[2], Amber E. Vater[3], Peter Wilson[4], Richard W. Mourne[5] and Jennifer L. Hill[5]

[1] Department of Geography, College of Science, Swansea University, Singleton Park, Swansea SA2 8PP, Wales, UK

[J.A.Matthews@Swansea.ac.uk; phone/fax +1633 413291]

[2] Department of Geological Sciences, University of Canterbury, Private Bag 4800, Christchurch 8140, New Zealand

[3] Natural Environment Research Council, Polaris House, Swindon SN2 8PP, UK

[4] Environmental Sciences Research Institute, School of Geography and Environmental Sciences, Ulster University, Cromore Road, Coleraine BT52 1SA, Northern Ireland, UK

[5] Department of Geography and Environmental Management, University of the West of England, Coldharbour Lane, Bristol BS16 1QY, UK

ABSTRACT

An index of the degree of rock-surface microweathering based on Schmidt hammer R-values is developed for use in the field without laboratory testing. A series of indices – I_2 to I_n , where n is the number of successive blows with the hammer – is first proposed based on the assumption that the R-values derived from successive impacts on the same spot on a weathered rock surface converge on the value characteristic of an unweathered surface of the same lithology. Of these indices, the I_5 index, which measures the difference between the mean R-value derived from first and fifth impacts as a proportion of the mean R-value from the fifth impact, is regarded as optimal: use of fewer impacts (e.g. in an I_2 index) underestimates the degree of weathering whereas use of more impacts (e.g. in an I_{10} index) makes little difference and is therefore inefficient and may also induce an artificial weakening of the rock. Field tests of these indices on weathered glacially-scoured bedrock outcrops of nine common metamorphic and igneous rock types from southern Norway show,

however, that even after ten impacts, successive R-values fail to approach the values characteristic of unweathered rock surfaces (e.g. bedrock from glacier forelands and road cuttings). An improved $*I_5$ index is therefore preferred, in which the estimated true R-value of an unweathered rock surface is substituted. Weathered rock surfaces exposed to the atmosphere for ~10,000 years in southern Norway exhibit $*I_5$ indices of 36-57%, values that reflect a similarly high degree of weathering irrespective of the rock type.

Key words: Rock microweathering indices, $*I_5$ index, Schmidt hammer R-values, metamorphic and igneous rocks, chemical weathering, Norway

1. Introduction

The degree to which a rock surface has been affected by microweathering on exposure to the atmosphere can be measured in a variety of ways (Aydin and Duzgoren-Aydin, 2002; Moses et al., 2014). Approaches range from the direct measurement of weight loss (Trudgill, 1975; Thorn et al., 2002) and rock-surface lowering (Dahl, 1967; André, 2002; Owen et al., 2007; Nicholson, 2008) to the measurement of weathering rinds (e.g. Chinn, 1981; Coleman and Pierce, 1981; Knuepfer, 1994; Birkeland and Noller, 2000; Oguchi, 2013) and the analysis of solutes in runoff (Darmody et al., 2000; Beylich et al., 2005). A further approach involves the use of Schmidt hammer rebound values (R-values), which measure rock hardness and hence are sensitive to rock weakening as a result of rock-surface weathering.

The Schmidt hammer was designed to test the hardness and strength of concrete (Schmidt, 1950). It has subsequently been widely used in rock mechanics (Hucka, 1965; Poole and Farmer, 1980; Aydin and Basu, 2005; Aydin, 2009) and adopted by geomorphologists who have explored its use in the context of the microweathering and dating of natural rock surfaces and building stone (e.g. Day and Goudie, 1977; McCarroll, 1994; Goudie, 2006, 2013; Nicholson, 2009; Matthews and Owen, 2011; Viles et al., 2011). This paper develops the approach further by focusing on the derivation and application of a quantitative weathering index from R-values, with the aim of providing a measure of the degree of weathering of rock surfaces that

is reliable, widely applicable, low cost and easy to use in the field. The index is evaluated with particular reference to common metamorphic and igneous rock types in alpine, subalpine and boreal zones in southern Norway.

2. Tested rock types and methods

2.1 Weathered and unweathered rock surfaces

Weathered and unweathered surfaces of nine different metamorphic and igneous rock types from the Jotunheimen, Jostedalsbreen, Breheimen and Reinheimen regions of southern Norway have been investigated. Identification of rock types was based on field observation combined with geological maps (Lutro and Tveten, 1996; Tveten et al., 1998). Named site locations are shown in Figures 1 and 2. The weathered surfaces are mostly glacially-scoured bedrock outcrops (e.g. Figure 3A), which were deglaciated following the late-Preboreal Erdalen Event, which consisted of two glacier re-advances at about 10,200 and 9700 cal. years BP (Dahl et al., 2002). This class of weathered surface includes all sites in Jotunheimen where pyroxene granulite gneiss (sampled in Gravdalen and Leirdalen) is the commonest rock type (Battey and McRitchie, 1973, 1975) but related gneisses with gabbroic textures (sampled near Bøverbreen and Leirbreen) and peridotite intrusions (sampled in Gravdalen; Figure 3B) also occur (Matthews and Owen, 2010, 2011).

Calcitic schist was sampled near Bøvertun, north of the Northwestern Boundary Fault of Jotunheimen and quartzitic calcitic schist at Attgløyma, a lake on the Sognefjell (Gibbs and Banham, 1979; Owen et al., 2006). At various sites around the Jostedalsbreen ice cap, granitic gneiss (Fåbergstølen and Jostedalen sites, both in upper Jostedalen), granite (Kvamsdalen, near Veitastrond) and augen gneiss (Loenvatnet) were sampled. Most of these sites have been used previously as control points of age ~10,000 years in studies of Schmidt hammer exposure-age dating (Matthews and Owen, 2010; Matthews and Wilson, 2015). Finally, migmatitic (banded) gneiss was sampled at Øyberget in upper Ottadalen and in Alnesdalen, south of Andalsnes in Møre og Romsdal. The Øyberget site involved boulders on the upper surface of a rock glacier which, on the basis of Schmidt hammer exposure-age dating

(Matthews et al., 2013) and unpublished cosmogenic isotope dating (Linge et al., submitted), stabilized in the early Holocene ~10,500 years ago. The Alnesdalen site involved boulders on a Younger Dryas end moraine, which dates from ~11,500 cal. years BP (Carlson et al. 1983; Matthews and Wilson, 2015).
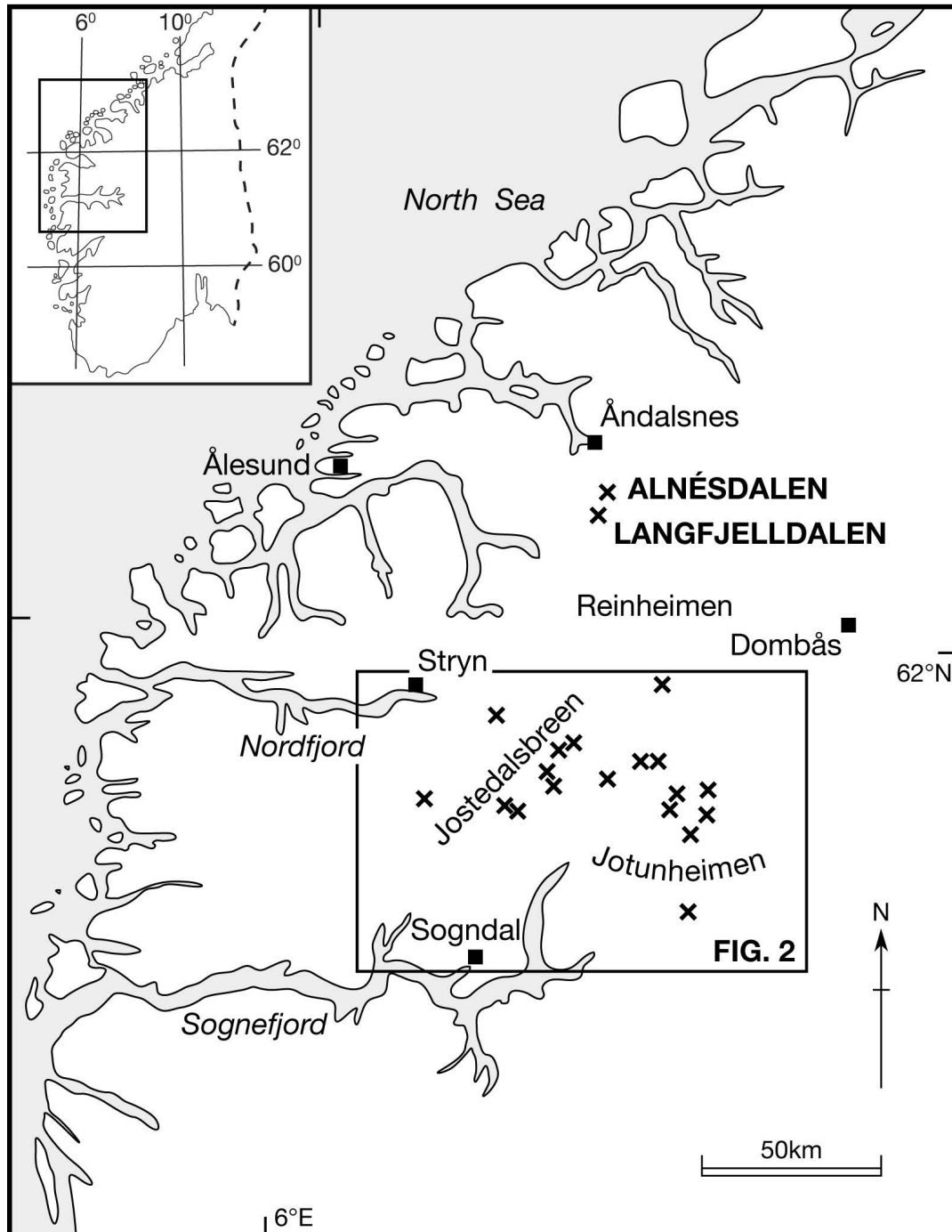

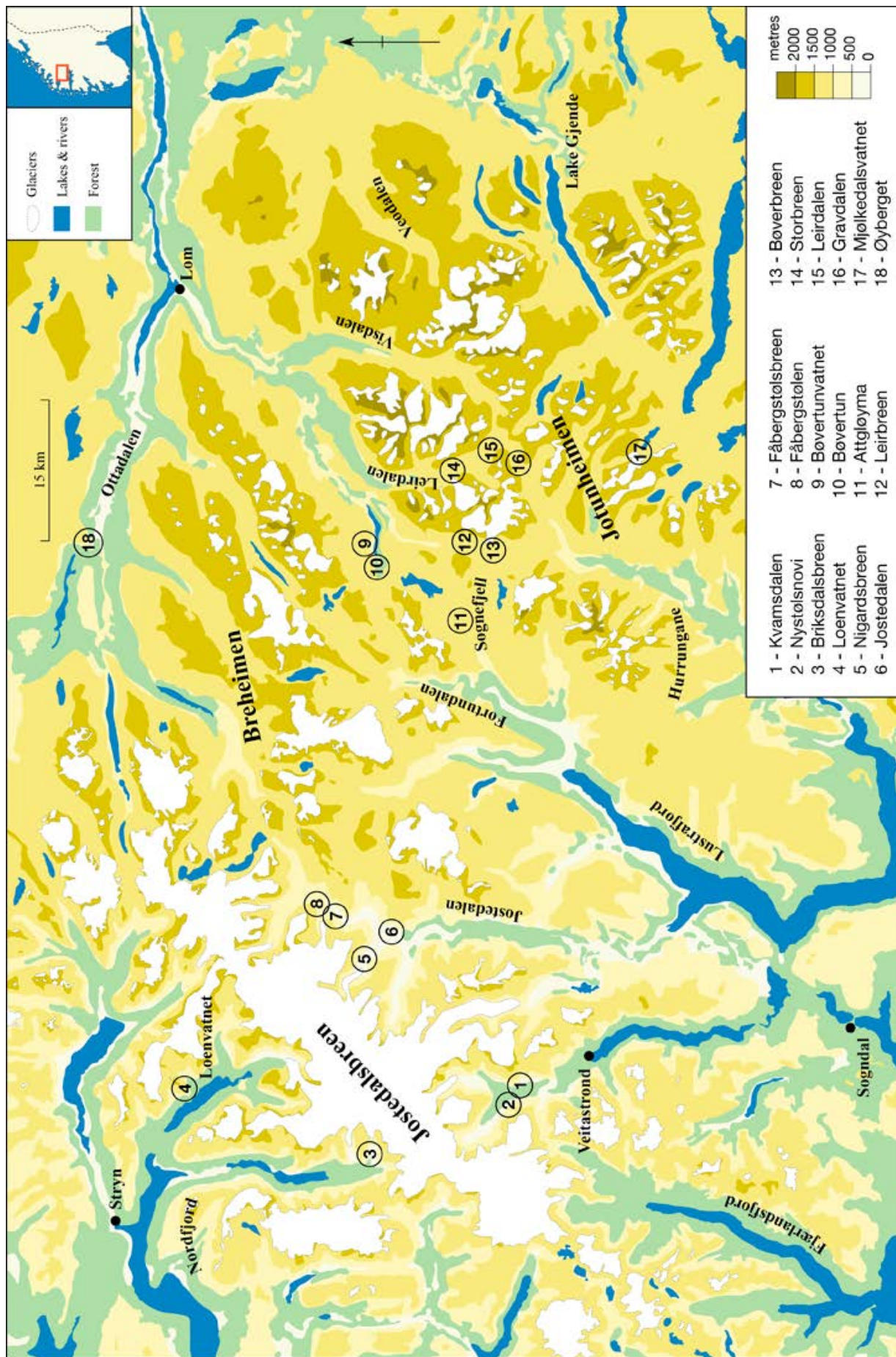Figure 1. Locations of field measurement sites (x) in southern Norway.

Figure 2. Detailed locations of field measurement sites in Jotunheimen, Jostedalsbreen and Breheimen regions.

Fresh, unweathered rock surfaces of several different types were sampled from each of the nine rock types. Where available, glacially-scoured bedrock outcrops from 'Little Ice Age' glacier forelands were used: in Jotunheimen, Storbreen (pyroxene-granulite gneiss and peridotite), Bøverbreen and Leirbreen (gabbroic gneiss), and Mjølkedalsbreen (peridotite); and at the Jostedalsbreen outlet glaciers of Nigardsbreen and Fåbergstølsbreen (granitic gneiss) and Briksdalsbreen (augen gneiss). Based on historical evidence and/or lichenometric dating, the bedrock outcrops selected were all deglacierized since the AD 1930s and therefore represent terrain ages of <90 years (cf. Bickerton and Matthews, 1992, 1993; Matthews, 2005).

Other types of unweathered rock surface used included: (1) glacially-abraded boulders embedded in fluted moraine on the Storbreen glacier foreland (pyroxene-granulite gneiss and peridotite) deglacierized since AD 1951; (2) anthropogenic bedrock surfaces in road cuttings (Gravdalen, pyroxene granulite-gneiss and peridotite; Bøvertunvatnet, calcitic schist), a road tunnel (Jostedalen, granitic gneiss) and a hydro-electric tunnel (Attgløyma, quartzitic calcitic schist), all excavated in the last 90 years; (3) boulders (Nystølsnovi, granite, and Langfjelldalen, migmatitic gneiss) produced by rockfalls that were observed to occur within the last 10 years (Matthews and Wilson, 2015); and (4) subsurface boulders excavated within the last three years in a road cutting in the toe of the Øyberget rock glacier (migmatitic gneiss). An example of an unweathered rock surface is shown in Figure 3C. The characteristics and appropriateness of these surfaces are discussed further below.

2.2 R-value measurements
Field measurements were made using a standard mechanical N-type Schmidt hammer (Proceq, 2004), which was periodically tested against the manufacturer's anvil to ensure no deterioration in R-values during the study. Successive impacts of the Schmidt hammer were made at particular points on the rock surfaces. Points were

Figure 3. A, a typical weathered glacially-scoured rock outcrop of granitic gneiss in Jostedalen; B, a weathered bedrock outcrop of peridotite in Gravdalen, Jotunheimen, showing five points on the rock surface where successive Schmidt-hammer impacts were made; C, an unweathered surface of pyroxene-granulite gneiss in a road cutting in Gravdalen showing three points where successive Schmidt-hammer impacts were made. Note Schmidt hammer for scale.

selected that avoided lichen and moss cover, edge effects, cracks and other visible structural weaknesses in the rock surface. Areas of water seepage were also avoided and all the measurements were made under dry weather conditions. Special attention was paid to ensuring successive blows were made at precisely the same point on the rock surface (see, for example, Figures 3B and 3C).

On weathered surfaces, 10 successive impacts were measured at each of 60 points (n = 600 Schmidt hammer impacts). Where weathered bedrock surfaces were involved, the 60 points were selected from at least three different outcrops or at least three different areas of the rock surface. Where weathered boulders were used, no more than five points were selected from each boulder ensuring that at least 12 boulders were sampled. As unweathered surfaces produced generally less variable R-values, five successive impacts were taken from each of 20 points on the unweathered rock surfaces (n = 100 Schmidt hammer impacts).

2.3 Derivation of microweathering indices

Indices were derived based on the increase in R-values from successive impacts of the Schmidt hammer on the same point of a weathered rock surface. The fact that R-values tend to increase with successive impacts, even on fresh rock surfaces, has been noted in previous investigations of the consistency and repeatability of Schmidt hammer measurements, which has led to various recommendations concerning the number of impacts necessary to determine a representative peak R-value that avoids any weathering effects (Hucka, 1965; Poole and Farmer, 1980; Aydin, 2009).

Nicholson (2009) showed that the difference between the first and second impact with a Schmidt hammer is a reflection of the degree of weathering of a weathered rock surface and suggested that the second impact approaches the R-value characteristic of the intact, unweathered rock. In effect, therefore, she proposed a simple index of the degree of weathering of the rock surface, $Rw_2 - Rw_1$, where Rw_1 is the mean R-value of first impacts and Rw_2 is the mean R-value of second impacts (our notation).

Matthews and Owen (2011) pointed out, however, that the second impact will

only approximate the R-value characteristic of unweathered rock if the first impact removes all traces of weathered material from the rock surface. The rise in R-value with further impacts after the second impact (Poole and Farmer, 1980; see also the results below) confirm, moreover, that the second impact is unlikely to provide a close approximation to the R-value characteristic of unweathered rock. Furthermore, progressively better indices of degree of weathering are likely to be produced by the use of the third and subsequent impacts as closer approximations to the R-value characteristic of the unweathered rock surface. Thus, an index based on $(Rw_2 - Rw_1)$ is merely the first in a series of indices culminating in $(Rw_n - Rw_1)$ based on the nth impact.

In order to take account of the effects of rock type on the R-value characteristic of unweathered rock, the differences between the mean R-values characteristic of the first to nth impacts can be expressed as percentages of the mean R-values characteristic of the nth impacts. The general formula for this series of potential indices therefore takes the form:

$$I_n = 100 \ (Rw_n - Rw_1) \ / \ Rw_n \tag{1}$$

Here, this series of indices is evaluated based on use of mean R-values from the second, fifth and tenth impacts:

$$I_2 = 100 \ (Rw_2 - Rw_1) \ / \ Rw_2 \tag{2}$$
$$I_5 = 100 \ (Rw_5 - Rw_1) \ / \ Rw_5 \tag{3}$$
$$I_{10} = 100 \ (Rw_{10} - Rw_1) \ / \ Rw_{10} \tag{4}$$

Although evaluation of only three of a potentially much larger number of indices may appear arbitrary, our results from the nine rock types from southern Norway, and comparison with previous work, justify this choice (see below).

However, even after the tenth impact, R-values characteristic of true, unweathered rock surfaces are not attained. Thus, although the I_5 index may provide an improvement on I_2 and is more efficient than I_{10}, it remains a relatively poor underestimate of the degree of weathering of the rock surfaces. Consequently, an

9

improved I_5 index ($*I_5$) is proposed, which combines efficiency with a reliable measure of the difference between R-values characteristic of the weathered and unweathered rock surface. This differs from the initial, uncorrected I_5 index in two respects. First, a correction factor ($Ru_5 - Rw_5$) is added to ($Rw_5 - Rw_1$), where Ru_5 is the mean R-value of the fifth impact from the independent unweathered rock surface of the same lithology. Second, Ru_5 is substituted for Rw_5 in the denominator. Thus,

$$*I_5 = 100 \ [(Rw_5 - Rw_1) + (Ru_5 - Rw_5)] \ / \ Ru_5 \tag{5}$$

This shortens to:

$$*I_5 = 100 \ (Ru_5 - Rw_1) \ / \ Ru_5 \tag{6}$$

Equation (6) describes the preferred index in a series of improved indices with the general formula:

$$*I_n = 100 \ (Ru_n - Rw_1) \ / \ Ru_n \tag{7}$$

Use of $*I_5$ in preference to other potential indices in the series $*I_2$ to $*I_n$ might again appear arbitrary but is justified by our results, which consistently show only slight differences between mean R-values associated with the fifth and subsequent impacts. Our use of the fifth impact is, moreover, compatible with its use in previously proposed indices. The improved $*I_5$ index is similar to the index of rock weathering (IRW) used by Matthews and Owen (2011) in relation to the Schmidt hammer and to several other indices proposed independently for related devices, such as the Equotip (Aoki and Matsukura, 2007; Yilmaz, 2013; Wilhelm et al., in press). It transpires that the improved $*I_5$ index is equivalent in concept to the deformation ratio (δ) of Aoki and Matsukura (2007), although the latter uses median R-values, and is expressed as a value between 0 and 1, and is close numerically to ($100 - *I_5$) if expressed as a percentage.

3. Results

3.1 Mean R-values from weathered rock surfaces

The effects of successive impacts on R-values associated with weathered surfaces of the nine rock types investigated from southern Norway are summarized in Table 1. The rock types in this table have been placed in descending order according to the mean R-value of the fifth impact (Rw_5) with replicate samples from four of the rock types listed separately. The 95% confidence intervals indicate both the variability and statistical significance of the differences between mean values. These data and the curves in Figures 4 and 5 show several general patterns:

- a clear trend of increasing mean R-values with successive impacts;
- consistent large and statistically significant increases in mean R-values between the first (Rw_1) and second (Rw_2) impacts;
- the lack of statistically significant differences between mean R-values after the fourth (Rw_4) or fifth (Rw_5) impacts as the curves level off;
- distinct differences in mean R-values between rock types, which tend to be maintained with successive impacts;
- excellent replication of results between the four rock types for which more than one sample is available (Figure 5).

3.2 Mean R-values from unweathered rock surfaces

Successive impacts on the unweathered rock surfaces (Table 2) yield generally less variable mean R-values and simpler patterns with a major difference between, on the one hand, the glacially-abraded surfaces (bedrock and boulders) and, on the other hand, the rockfall and rockglacier boulders, and bedrock in road cuttings and tunnel walls. Notable patterns, illustrated in Figure 6, include:

- the absence of any statistically significant trend in mean R-values associated with successive impacts on the glacially-abraded surfaces;
- remarkably similar mean R-values characteristic of the glacially-abraded surfaces, irrespective of rock type;
- consistent (but often not statistically significant) differences between mean Ru_1 and Ru_2 values associated with rockfall boulders and anthropogenic

bedrock surfaces; mean Ru_3 and subsequent values are, however, often significantly different from mean Ru_1 values.

- non-statistically significant differences where the data enable mean Ru_5 values for glacially-abraded surfaces to be compared with rockfall boulders or anthropogenic bedrock surfaces from the same rock type;

- mean Ru_5 values that are usually statistically significantly greater than mean Rw_5 values (irrespective of rock type or surface type).

3.3 The weathering indices

The I_2, I_5 and I_{10} indices, and the improved $*I_5$ index, are summarized in Table 3. Important features of these results are as follows:

- the consistent increase in the percentage value of the indices from I_2 to I_{10} with the improved $*I_5$ index yielding the highest value, which applies to all rock types;

- the large differences between the values of I_2 and I_5 (average difference 8.9% across all 13 samples from the nine rock types), which contrast strongly with the much smaller average difference between I_5 and I_{10} (1.7%) and reflect the large differences between the mean R-values of Rw_1 and Rw_2 evident in Figure 4.

- the even larger differences between the I_5 index and the improved $*I_5$ index (average difference 11.7%), which reflect the inadequacy of Rw_5 values (and also Rw_{10} values) as approximations of R-values characteristic of unweathered rock surfaces, and the improvement brought about by using Ru_5 values;

- the relatively small range (36.1-56.6%) exhibited by the improved $*I_5$ index between rock types.
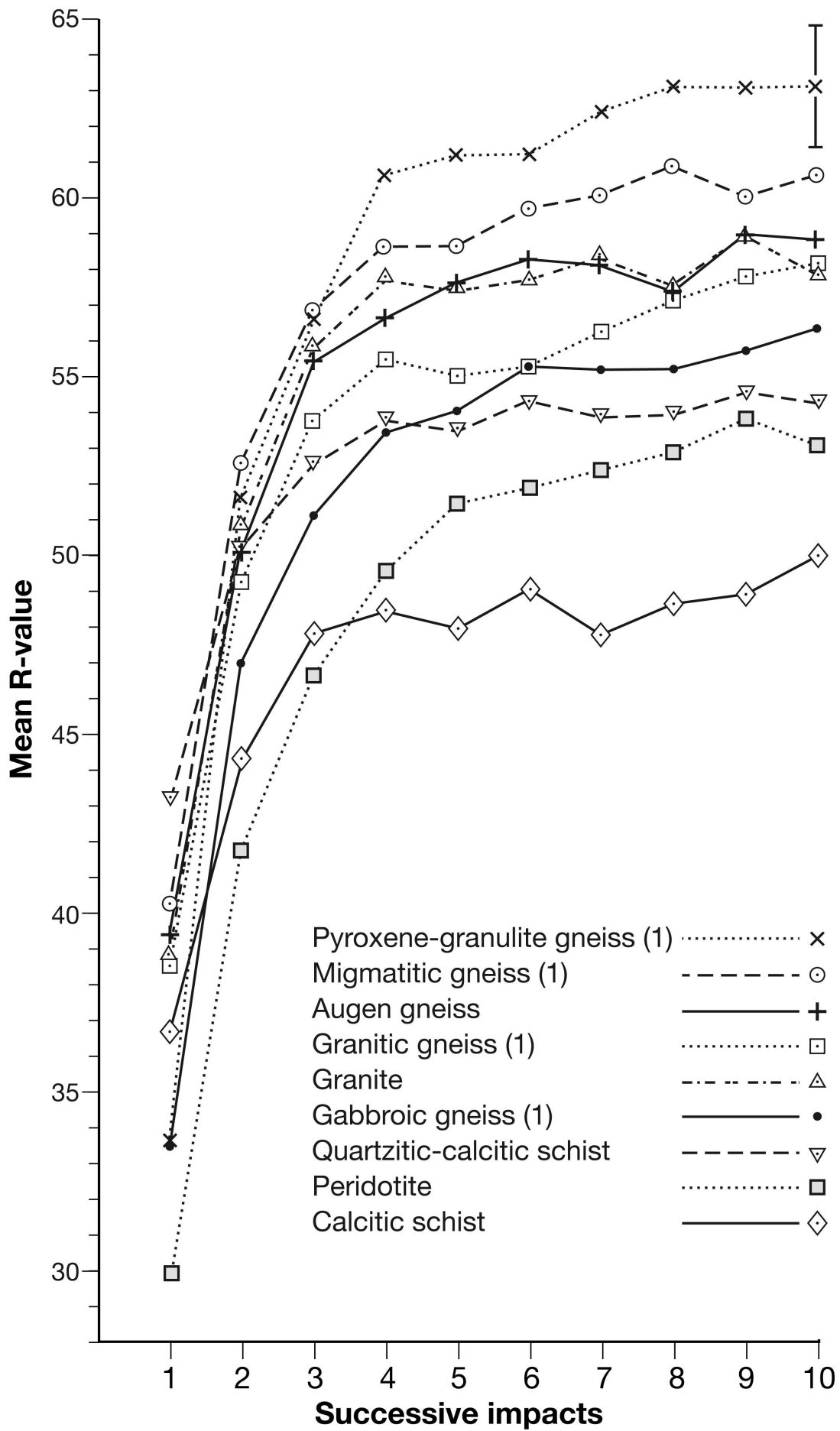
Figure 4. Mean Schmidt hammer R-values for successive impacts on the weathered surfaces of nine rock types. A representative 95% confidence interval is shown (all confidence intervals are given in Table 1).

Table 1 Schmidt hammer R-values (mean ± 95% confidence interval; n = 60) for successive impacts (Rw_1 to Rw_{10}) from weathered bedrock surfaces of age ~10,000 years (* Øyberget rock-glacier boulders).

| Rock type	Location	Rw_1	Rw_2	Rw_3	Rw_4	Rw_5	Rw_6	Rw_7	Rw_8	Rw_9	Rw_{10}
Pyroxene-granulite gneiss	Gravdalen	33.8±2.4	51.7±1.8	56.7±1.6	60.7±1.1	61.2±0.9	61.2±1.2	62.4±1.2	63.1±1.0	63.0±1.1	63.1±1.6
Migmatitic gneiss	Alnesdalen	40.3±2.4	52.6±2.4	56.9±1.8	58.7±1.6	58.7±1.9	59.7±1.8	60.1±1.7	60.9±1.3	60.0±1.7	60.6±1.5
Augen gneiss	Loenvatnet	39.4±2.0	50.1±2.5	55.5±1.7	56.7±1.9	57.6±1.7	58.3±1.6	58.2±1.6	57.4±1.6	59.1±1.6	59.0±1.7
Granite	Kvamsdalen	38.9±1.7	50.8±2.0	55.9±1.7	57.8±1.6	57.6±1.7	57.8±1.9	58.4±1.6	57.6±2.3	59.2±1.4	57.9±1.6
Granitic gneiss	Fåbergstølen	38.5±1.9	49.3±2.0	53.8±2.0	55.5±1.4	55.0±2.0	55.3±1.6	56.3±1.6	57.2±1.6	57.8±1.3	58.1±1.3
Gabbroic gneiss	Bøverbreen	33.6±2.4	47.1±2.4	51.2±2.2	53.5±1.8	54.1±1.8	55.3±1.7	55.3±1.6	55.2±1.9	55.7±1.7	56.4±1.5
Quartzitic calcitic schist	Attgløyma	43.2±1.5	50.2±1.3	52.6±1.4	53.8±1.3	53.5±1.7	54.3±1.4	53.9±1.1	54.0±1.4	54.6±1.3	54.3±1.4
Peridotite	Gravdalen	29.4±1.9	41.8±2.5	46.6±2.0	48.6±2.1	51.5±1.6	51.9±1.7	52.4±1.6	52.9±1.5	53.9±1.4	53.2±1.4
Calcitic schist	Bøvertun	36.7±2.1	44.3±2.6	47.8±2.7	48.5±2.6	48.0±2.7	49.1±2.6	47.8±2.7	48.7±2.5	48.9±2.4	50.0±2.5
Pyroxene-granulite gneiss	Leirdalen	36.1±2.1	54.0±1.4	56.3±1.7	58.7±1.3	59.7±1.2	60.4±1.3	59.7±1.6	61.2±1.2	61.2±1.4	60.6±1.8
Migmatitic gneiss	Øyberget*	43.0±2.6	53.1±2.5	56.0±1.8	57.9±1.5	59.1±1.7	59.6±1.4	59.6±1.3	59.8±1.6	60.6±1.5	59.4±1.8
Granitic gneiss	Jostedalen	41.6±1.9	50.9±2.1	55.1±1.7	55.1±2.4	58.1±1.7	57.6±1.5	58.0±1.7	58.2±1.6	58.3±1.4	59.1±1.5
Gabbroic gneiss	Leirbreen	35.5±2.4	47.0±2.7	50.8±2.3	53.5±1.7	55.0±1.7	55.8±1.8	56.0±1.5	57.0±1.4	55.8±2.0	56.9±1.3
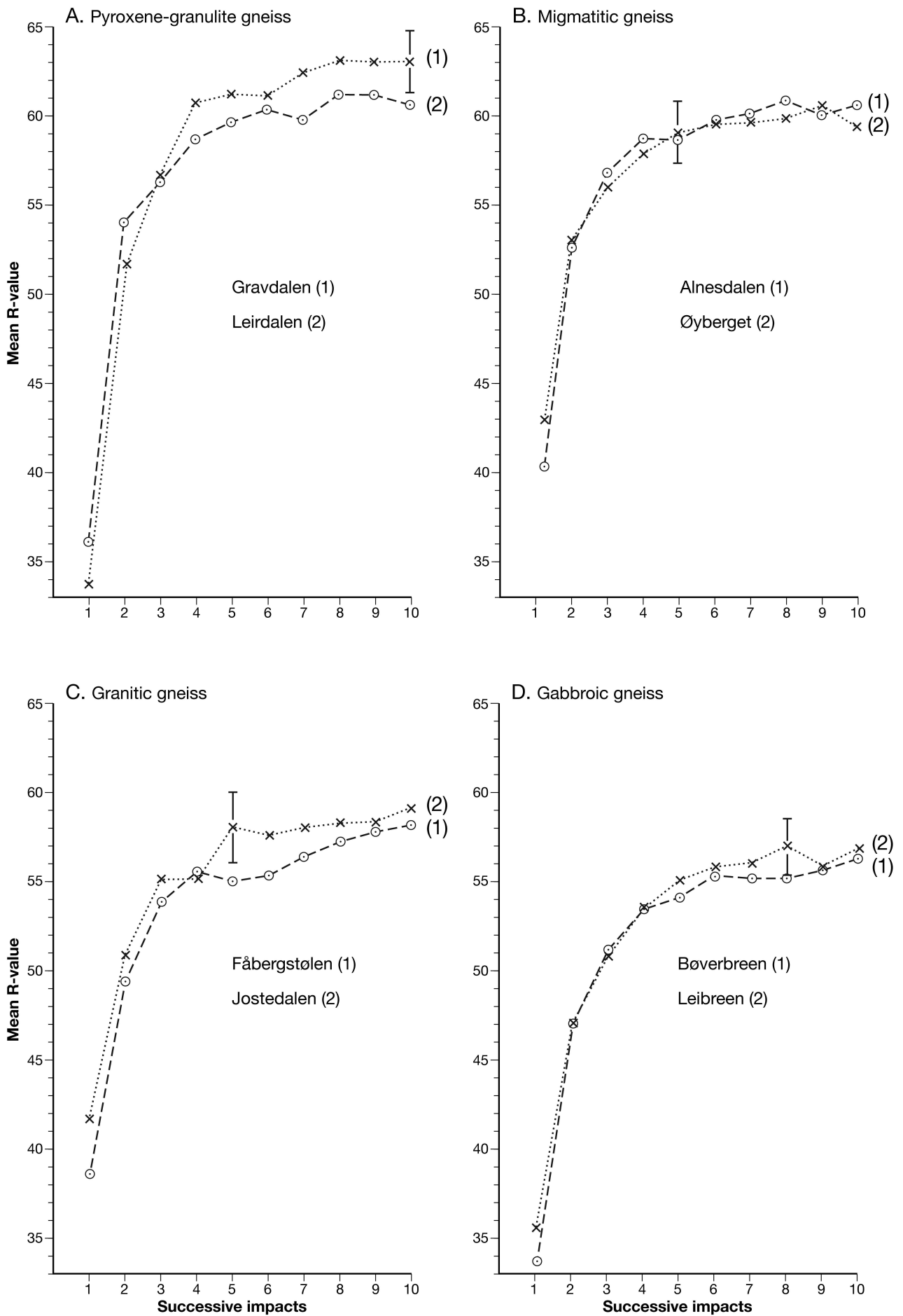
Figure 5. Replication of mean Schmidt hammer R-values for successive impacts on the weathered surfaces of four rock types (representative 95% confidence intervals are shown).

Table 2 Schmidt hammer R-values (mean ± 95% confidence interval; n = 20) for successive impacts (Ru_1 to Ru_5) from unweathered rock surfaces.

Rock type and location	Ru_1	Ru_2	Ru_3	Ru_4	Ru_5	Surface type
Pyroxene-granulite gneiss						
Gravdalen	61.3±1.2	63.7±1.4	65.4±1.0	65.2±1.0	65.4±0.9	road-cutting bedrock
Storbreen glacier foreland	67.5±1.7	67.8±1.9	67.2±1.7	66.9±2.2	67.3±1.6	glacially-abraded bedrock
Storbreen glacier foreland	67.0±1.2	66.6±1.2	67.9±1.2	67.4±1.5	67.2±1.5	glacially-abraded boulders
Migmatitic gneiss						
Langfjelldalen	60.6±3.0	64.9±1.7	64.7±3.0	66.6±1.8	67.4±1.5	rockfall boulders
Øyberget	61.7±3.2	65.6±2.8	66.9±2.0	67.1±1.5	65.4±3.1	rock-glacier boulders (potassium-feldspar bands)
Øyberget	63.6±2.5	68.8±1.1	69.3±1.7	68.8±1.8	69.5±1.1	rock-glacier boulders (biotite-mica bands)
Augen gneiss						
Briksdalsbreen glacier foreland	67.0±1.3	68.6±1.3	68.6±1.5	68.2±1.3	67.5±1.9	glacially-abraded bedrock
Granite						
Nystølsnovi	57.1±2.5	61.7±2.4	63.7±2.3	64.0±2.0	64.2±2.0	rockfall boulders
Granitic gneiss						
Fåbergstølsbreen glacier foreland	68.2±1.7	69.0±1.4	69.6±1.7	69.3±1.6	68.0±2.1	glacially-abraded bedrock
Nigardsbreen glacier foreland	69.5±1.9	69.8±2.3	71.3±1.2	70.3±1.7	70.0±1.7	glacially-abraded bedrock
Fåberstølen	66.9±1.7	68.5±1.5	69.5±1.3	68.9±1.6	68.6±1.6	road-tunnel bedrock
Gabbroic gneiss						
Bøverbreen glacier foreland	66.1±2.5	68.2±2.1	69.5±1.3	68.9±2.1	69.3±1.4	glacially-abraded bedrock
Leirbreen glacier foreland	66.7±1.1	67.3±1.1	67.4±1.1	67.0±1.1	67.9±1.6	glacially-abraded bedrock
Quartzitic calcitic schist						
Attgløyma	53.6±3.1	56.4±2.7	57.1±3.2	57.9±2.9	58.6±2.6	hydro-electric tunnel bedrock
Peridotite						
Gravdalen	63.0±1.6	67.5±2.0	66.6±2.1	67.3±2.1	67.3±2.1	road-cutting bedrock
Storbreen glacier foreland	67.9±2.8	70.0±1.7	69.4±2.4	67.8±2.8	67.3±3.0	glacially-abraded boulders
Mjølkedalsbreen glacier foreland	67.8±0.8	68.2±0.9	68.4±0.3	68.3±0.7	68.8±0.8	glacially-abraded bedrock
Calcitic schist						
Bøvertunvatnet	54.4±3.7	54.4±3.6	56.5±3.1	55.6±3.9	57.4±3.0	road-cutting bedrock

4. Discussion

The indices of degree of microweathering developed in this paper (I2, I5, I10 and the improved *I5 index) are measures of the loss of compressional strength of a rock surface as a result of weathering standardized with respect to the estimated strength of unweathered rock of the same lithology. Expressed as a percentage, 0% is the expected value of each index for an unweathered rock of any lithology whereas 100% is the corresponding theoretical value for a surface that has completely disintegrated and hence has been weakened by weathering to such an extent as to exhibit zero strength. 'Indices of rock-surface weakening' is therefore an alternative term, which has been recognized in relation to earlier related indices based on the physical strength of rock rather than its chemical make-up (Nicholson, 2009; Matthews and Owen, 2011).

When applied to a particular weathered rock surface, the values of all these indices are highly dependent on the mean R-value of the first impact (Rw1). Many forms of microweathering are potential influences on Rw1, including chemical weathering, biochemical weathering, biological mechanical weathering and microgelifraction/microgelivation (Nicholson, 2009; Matthews and Owen, 2011). The extent to which Rw1 differs from the estimated mean R-value for unweathered rock of the same lithology (Rw5 or Ru5) is affected especially by the collapse of protuberances that result from differential weathering of minerals at the rock surface. This is particularly noticeable with respect to the Rw1 values for peridotite, pyroxene-granulite gneiss and gabbroic gneiss (Table 1; Figures 3B and 4). Where the protuberances are themselves strong and hard, they resist subsequent impacts and result in a relatively slow increase in the R-values from impacts Rw3 to Rw10 (see again the curve for peridotite in Figure 4).

Although indices I2 to I10 may be viewed as progressively closer approximations to the best index of its type, even I10 is unsatisfactory because Rw10 is not a close estimate of the mean R-value characteristic of unweathered rock surfaces. A number of factors account for the fact that Rw10 underestimates the true mean R-value of intact, unweathered rock as determined directly in this study (Table 2). These factors include the accumulation of pulverized rock material beneath the hammer, penetration of microweathering effects (especially chemical weathering) deep below the rock surface, and/or the weakening of otherwise intact rock at depths below the weathered surface by shock effects from a large numbers of impacts. Whereas pulverized rock material could be removed by careful cleaning of the rock surface
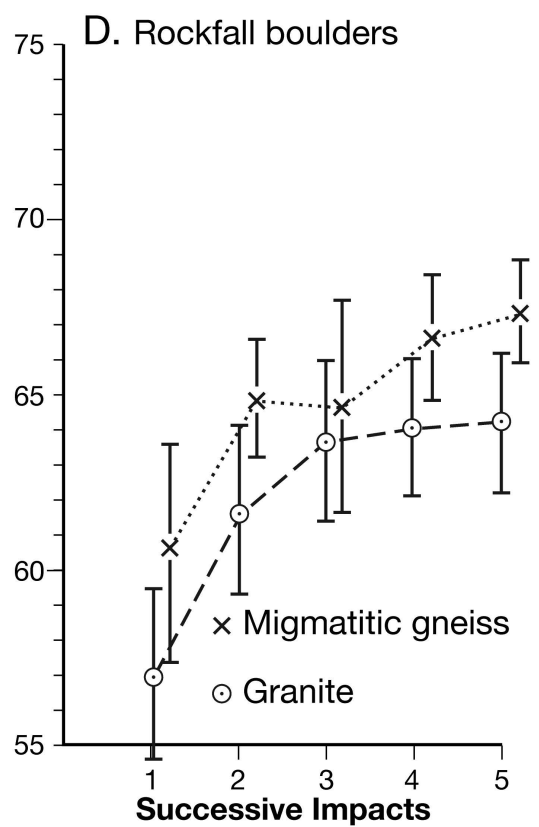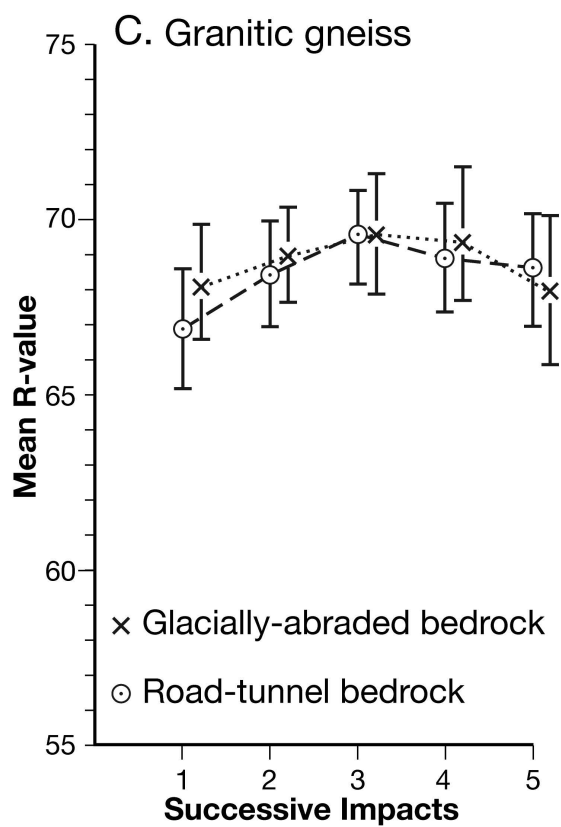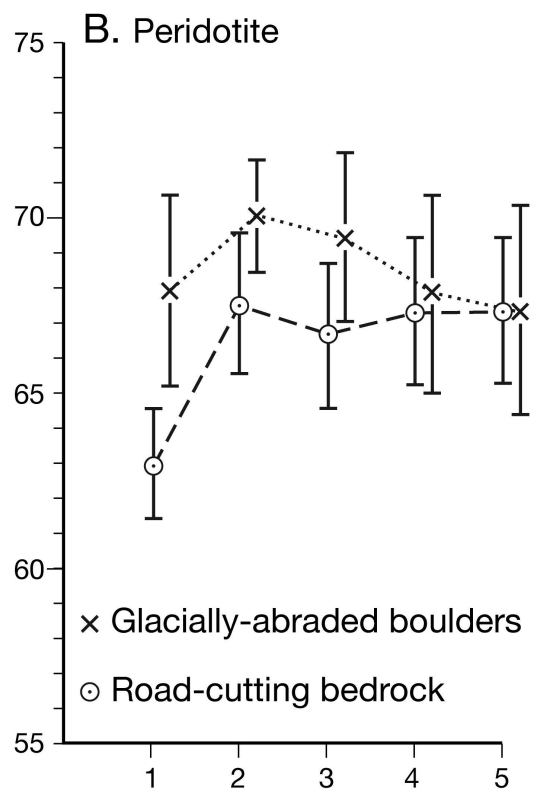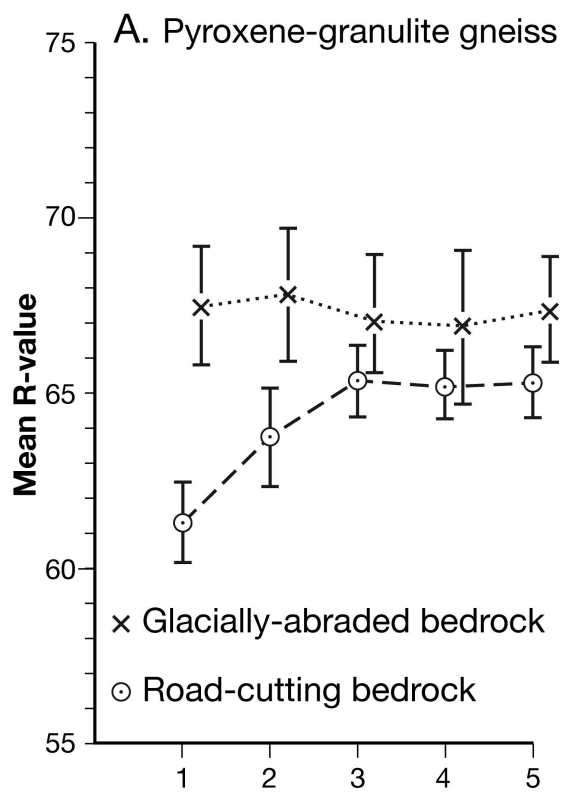
Figure 6. Mean Schmidt hammer R-values (± 95% confidence intervals) for successive impacts on selected unweathered rock surfaces.

after each successive impact, it is not possible to control effectively for the other factors. Thus, it is unlikely that a close approximation to the true mean R-value characteristic of unweathered rock can be found from weathered rock surfaces, no matter how many successive impacts are made.

A major advantage of the improved $*I_5$ index in its shortened form (equation 6) over the uncorrected indices is that it does not require measurement of any impacts on the weathered rock surface apart from Rw_1. Futhermore, by replacing Rw_5 with the fifth impact from the unweathered rock surface (Ru_5), the improved $*I_5$ index uses a very close approximation to the true mean R-value of the unweathered rock surface. In turn, Ru_5 can be determined accurately from both natural and anthropogenic surfaces that have been recently exposed, thus avoiding the need for laboratory testing of prepared unweathered rock specimens.

There is no advantage in using Ru_5 rather than Ru_1 if the unweathered rock surface is a smooth, glacially-abraded surface because the first impacts on these surfaces do not differ from successive impacts. In relation to rockfall boulders and bedrock surfaces in road cuttings or tunnels, however, Ru_1 should not be used because the first impact on these surfaces tends to yield a relatively low R-value (Table 3) because of higher surface roughness. Such roughness effects are only removed after further impacts (usually less than five; Table 2).

Thus, the improved $*I_5$ index does not suffer the main limitation of the uncorrected I_5 index (namely, that Rw_5 is a poor approximation of the true mean R-value of the unweathered rock surface). An improved $*I_{10}$ index would, moreover, yield little or no additional benefit because the tenth impact from an unweathered rock surface (Ru_{10}) would not be expected to differ significantly from Ru_5. The improved $*I_5$ index is therefore not only reliable but efficient, requiring a minimum of field measurements. Perhaps the main limitation of this method as a means to quantify degree of weathering is the practical one of obtaining representative and comparable unweathered rock surfaces.

The relatively narrow range of 36.1-56.6% between rock types in the value of the improved $*I_5$ index (Table 3) may be interpreted as indicating that the various

Table 3 Indices of degree of weathering from Schmidt-hammer R-values for weathered rock surfaces

Rock type	Location	Rw_5-Rw_1	I_2 (%)	I_5 (%)	I_{10} (%)	Ru_5-Rw_5	Improved $*I_5$ (%)
Pyroxene-granulite gneiss	Gravdalen	27.4	34.6	44.8	46.5	4.2	48.3
Migmatitic gneiss	Alnesdalen	18.4	23.4	31.3	33.5	8.7	40.2
Augen gneiss	Loenvatnet	18.2	21.4	31.6	33.3	9.9	41.6
Granite	Kvamsdalen	18.7	23.4	32.4	32.8	6.6	39.4
Granitic gneiss	Fåbergstolen	16.5	21.9	29.9	33.8	13.3	43.6
Gabbroic gneiss	Boverbreen	20.5	28.5	37.8	40.3	15.2	51.5
Quartzitic calcitic schist	Attgløyma	10.3	13.9	19.2	20.4	14.4	36.4
Peridotite	Gravdalen	22.1	29.7	42.9	44.7	16.3	56.6
Calcitic schist	Bovertun	11.3	17.2	23.5	25.1	9.4	36.1
Pyroxene-granulite gneiss	Leirdalen	23.6	33.1	39.6	40.5	7.6	47.6
Migmatitic gneiss	Øyberget*	16.1	19.0	27.2	27.6	8.4	36.2
Granitic gneiss	Jostedalen	16.5	18.3	28.4	29.7	11.9	40.6
Gabbroic gneiss	Leirbreen	19.5	16.7	25.3	24.7	12.9	47.7

tested rock types exhibit quite similar degrees of weathering when the initial strength of the unweathered rock is taken into account. As most of these rock surfaces had been subject to weathering for about $10,000 \pm 500$ years (the exception being the Alnesdalen site involving migmatitic gneiss, which has been exposed to weathering for ~11,500 years), these index values indicate similar average weathering rates of 3.6-5.7% per 1000 years.

5. Conclusion

(1) The improved $*I_5$ index, $100 \, (Ru_5 - Rw_1) \, / \, Ru_5$, which has a potential range of 0 to 100%, provides a field measure of the degree of microweathering of a rock surface from Schmidt-hammer R-values. It measures the difference between the mean R-value sampled from the weathered rock surface (Rw_1) and the higher mean R-value characteristic of the fifth successive impact taken from the same spot on an unweathered rock surface of the same lithology (Ru_5). It therefore reflects the reduction in compressional strength of the rock surface as a result of weathering *relative* to the strength of the unweathered rock.

(2) This index improves on a series of indices (I_2 to I_n) derived from successive impacts on the weathered rock surface (Rw_1 to Rw_n). All indices in the series assume that the *n*th impact approximates the R-value characteristic of unweathered rock. Field tests on glacially-scoured bedrock outcrops of nine common metamorphic and igneous rock types from southern Norway, which were deglaciated between ~11,500 and 9700 years ago, demonstrate that this assumption is incorrect.

(3) The improved $*I_5$ index yielded values of 36-57% for the highly weathered metamorphic and igneous rock surfaces tested. It represents a substantial improvement on the uncorrected indices because it effectively corrects for the strength of the initially unweathered rock. It is, moreover, relatively easy to measure and Ru_5 can be obtained from a variety of unweathered natural and anthropogenic rock surfaces (e.g. glacially-abraded bedrock and boulders on glacier forelands, or bedrock exposed in modern road cuttings and tunnels) without the requirement for laboratory testing of rock specimens.

Acknowledgements

References

André, M.F., 2002. Rates of postglacial rock weathering on glacially scoured outcrops (Abisko-Riksgrånsen area, 68°N). *Geografiska Annaler* 64A, 139-150.

Aoki, H., Matsukura, Y., 2007. A new technique for non-destructive field measurement of rock-surface strength: an application of the Equotip hardness tester to weathering studies. *Earth Surface Processes and Landforms* 32, 1759-1769.

Aydin, A., 2009. ISRM suggested method for determination of the Schmidt hammer rebound hardness: revised version. *International Journal of Rock Mechanics and Mining Sciences* 46, 627-634.

Aydin, A., Basu, A., 2005. The Schmidt hammer in rock material characterization. *Engineering Geology* 81, 1-14.

Aydin, A., Duzgoren-Aydin, N.S., 2002. Indices for scaling and predicting weathering-induced changes in rock properties. *Environmental and Engineering Geoscience* 8, 121-135.

Battey, M.H., McRitchie, W.D., 1973. A geological traverse across the pyroxene-granulites of Jotunheimen in the Norwegian Caledonides. *Norsk Geologisk Tidsskrift* 53, 237-265.

Battey, M.H., McRitchie, W.D., 1975. The petrology of the pyroxene-granulite facies

rocks of Jotunheimen. *Norsl Geologisk Tidsskrift* 55, 1-49.

Beylich, A.A., Molau, U., Luthbom, K., Gintz, D., 2005. Rates of chemical and mechanical fluvial denudation in an Arctic oceanic periglacial environment, Latnjavagge drainage basin, northernmost Swedish Lapland. *Arctic, Antarctic and Alpine Research* 37, 75-87.

Bickerton, R.J., Matthews, J.A., 1992. On the accuracy of lichenometric dates: an assessment based on the 'Little Ice Age' moraine sequence of Nigardsbreen, southern Norway. *The Holocene* 2, 227-237.

Bickerton, R.J., Matthews, J.A., 1993. 'Little Ice Age' variations of outlet glaciers from the Jostedalsbreen ice-cap, southern Norway: a regional lichenometric-dating study of ice-marginal moraine sequences and their climatic significance. *Journal of Quaternary Science* 8, 45-66.

Birkeland, P.W., Noller, J.S., 2000. Rock and mineral weathering. In: Noller, J.S., Sowers, J.M., Lettis, W.R. (Eds.), *Quaternary Geochronology: Methods and Applications*. American Geophysical Union, Washington DC, pp. 293-312.

Carlson, A.B., Sollid, J.L., Torp, B., 1983. *Valldal Kvartaergeologi og geomorphologie, 1319IV [Valldal Quaternary Geology and Geomorphology, Sheet 1319 IV] 1:50,000.* Geografisk Institutt, Universitet I Oslo, Oslo.

Chinn, T.J.H., 1981. Use of rock weathering-rind thickness for Holocene absolute age-dating in New Zealand. *Arctic and Alpine Research* 13, 33-45.

Coleman, S.M., Pierce, K.L., 1981. Weathering rinds on andesitic and basaltic stones as a Quaternary age indicator, western United States. *United States Geological Survey Professional Paper* 1210, 1-54.

Dahl, R., 1967. Post-glacial micro-weathering of bedrock surfaces in the Narvik district of Norway. *Geografiska Annaler* 49A, 155-166.

Dahl, S.O., Nesje, A., Lie, Ø., Fjordheim, K., Matthews, J.A., 2002. Timing, equilibrium-line altitudes and climatic implications of two early-Holocene glacier readvances during the Erdalen Event at Jostedalsbreen, western Norway. *The Holocene* 12, 17-25.

Darmody, R.G., Thorn, C.E., Harder, R.L., Schlyter, J.P.L., Dixon, J.C., 2000. Weathering implications of water chemistry in an arctic-alpine environment, northern Sweden. *Geomorphology* 34, 89-100.

Day, M.J., Goudie, A.S., 1977. Field assessment of rock hardness using the Schmidt hammer. *British Geomorphological Research Group Technical Bulletin* 18, 19-29.

Gibbs, A.D., Banham, P.H., 1979. *Sygnefjell, Berggrunnsgeologisk kart 1518 III, 1:50,000*. Norges Geologiske Undersøkelse, Trondheim.

Goudie, A.S., 2006. The Schmidt hammer in geomorphological research. *Progress in Physical Geography* 30, 703-718.

Goudie, A.S., 2013. The Schmidt hammer and related devices in geomorphological research. In: Kennedy, D.M. Switzer, A. (Eds.), *Treatise on Geomorphology, Volume 14: Methods in Geomorphology*. Academic Press-Elsevier, Amsterdam, pp. 338-345.

Hucka, V.A., 1965. A rapid method for determining the strength of rocks. *International Journal of Rock Mechanics and Mining Sciences* 2, 127-134.

Knuepfer, P.L.K., 1994. Use of rock weathering rinds in dating geomorphic surfaces. In Beck, C. (Ed.), *Dating in Exposed and Surface Contexts*. University of New Mexico Press, Albuquerque, pp. 15-28.

Linge, H., Nesje, A., Matthews, J.A., Fabel, D., Xu, S., (submitted) [10]Be surface exposure ages from relict talus-derived rock glacier lobes at Øyberget, upper Ottadalen, southern Norway. *Quaternary Geochronology*.

Lutro, O., Tveten, E., 1996. *Geologisk kart over Norge, berggrunskart Årdal*

[Geological map of Norway: bedrock map, Årdal sheet] 1:250,000. Norges Geologiske Undersøkelse, Trondheim.

Matthews, J.A., 2005. 'Little Ice Age' glacier variations in Jotunheimen, southern Norway: a study in regionally-controlled lichenometric dating of recessional moraines with implications for climate and lichen growth rates. *The Holocene* 15, 1-19.

Matthews, J.A., Owen, G., 2010. Schmidt-hammer exposure-age dating: developing linear age-calibration curves using Holocene bedrock surfaces from the Jotunheimen-Jostedalsbreen regions of southern Norway. *Boreas* 39, 105-115.

Matthews, J.A., Owen, G., 2011. Holocene chemical weathering, surface lowering and rock weakening rates on glacially eroded bedrock surfaces in an alpine periglacial environment, Jotunheimen, southern Norway. *Permafrost and Periglacial Processes* 22, 279-290.

Matthews, J.A., Wilson, P., 2015. Improved Schmidt-hammer exposure ages for active and relict pronival ramparts in southern Norway, and their palaeoenvironmental implications. *Geomorphology* 246, 7-21.

Matthews, J.A., Nesje, A., Linge, H., 2013. Relict talus-foot rock glaciers at Øyberget, upper Ottadalen, southern Norway: Schmidt-hammer exposure ages and palaeoenvironmental implications. *Permafrost and Periglacial Processes* 24, 336-346.

McCarroll, D., 1994. The Schmidt hammer as a measure of the degree of rock surface weathering and terrain age. In; Beck, C. (Ed.), *Dating in Exposed and Surface Contexts*. University of New Mexico Press, Albuquerque, pp. 641-651.

Moses, C., Robinson, D., Barlow, J., 2014. Methods for measuring rock surface weathering and erosion: a critical review. *Earth-Science Reviews* 135, 141-161.

Nicholson, D.T., 2008. Rock control on microweathering of bedrock surfaces in a periglacial environment. *Geomorphology* 101, 655-665.

Nicholson, D.T., 2009. Holocene microweathering rates and processes on ice-eroded bedrock, Røldal area, Hardangervidda, southern Norway. In: Knight, J., Harrison, S. (Eds.), *Periglacial and Paraglacial Processes and Environments*, The Geological Society, London: Special Publication 320, pp. 29-49.

Oguchi, C.T., 2013. Weathering rinds: formation, processes and weathering rates. In; Pope, G.A. (Ed.), *Treatise on Geomorphology, Volume 4: Weathering and Soils Geomorphology.* Academic Press-Elsevier, Amsterdam, pp. 98-110.

Owen. G., Matthews, J.A., Shakesby, R.A., 2006. Rapid Holocene chemical weathering on a calcitic lake shoreline in an alpine periglacial environment: Attgløyma, Sognefjell, southern Norway. *Permafrost and Periglacial Processes* 17, 3-12.

Owen. G., Matthews, J.A., Albert, P.G., 2007. Rates of Holocene chemical weathering, 'Little Ice Age' glacial erosion, and implications for Schmidt-hammer dating at a glacier-foreland boundary, Fåbergstølsbreen, southern Norway. *The Holocene* 17, 829-834.

Poole, R.W., Farmer, I.W., 1980. Consistency and repeatability of Schmidt hammer rebound data during field testing. *International Journal of Rock Mechanics and Mining Sciences and Geomechanics Abstracts* 17, 167-171.

Proceq, 2004. *Operating instructions Betonprüfhammer N/NR- L/LR.* Proceq SA, Schweizenbach.

Schmidt, E., 1950. Der Beton-Prüfhammer. *Schweizer Baublatt, Zürich* 68(28) 1950, 378.

Thorn, C.E., Darmody, R.G., Dixon, J.C., Schlyter, P., 2002. Weathering rates of machine-polished rock discs, Kärkevagge, Swedish Lapland. *Earth Surface Processes and Landforms* 27, 831-845.

Trudgill, S.T., 1975. Measurement of erosional weight-loss of stone tablets. *British Geomorphological Research Group Technical Bulletin* 17, 13-19.

Tveten, E., Lutro, O., Thorsnes, T., 1998. *Geologisk kart over Norge, berggrunskart Ålesund [Geological map of Norway: bedrock map, Ålesund sheet] 1:250,000.* Norges Geologiske Undersøkelse, Trondheim.

Viles, H., Goudie, A., Grab, S., Lalley, J., 2011. The use of the Schmidt hammer and Equotip for rock hardness assessment in geomorphology and heritage science: a comparative analysis. *Earth Surface Processes and Landforms* 36, 320-333.

Wilhelm, K., Viles, H., Burke, Ó., (in press) Low impact surface hardness testing (Equotip) on porous rock and stone – advances in methodology with implications for rock weathering and stone deterioration research. *Earth Surface Processes and Landforms* DOI:10.1002/esp.3882

Yilmaz, N.G., 2013. The influence of testing procedures on uniaxial compressive strength prediction on carbonate rocks from Equotip hardness tester (EHT) and proposal of new testing methodology: hybrid dynamic hardness (HDH). *Rock Mechanics and Rock Engineering* 46, 95-106.

Figure captions

Figure 1. Locations of field measurement sites (x) in southern Norway.

Figure 2. Detailed locations of field measurement sites in Jotunheimen, Jostedalsbreen and Breheimen regions.

Figure 3. A, a typical weathered glacially-scoured rock outcrop of granitic gneiss in Jostedalen; B, a weathered bedrock outcrop of peridotite in Gravdalen, Jotunheimen, showing five points on the rock surface where successive Schmidt-hammer impacts were made; C, an unweathered surface of pyroxene-granulite gneiss in a road cutting in Gravdalen showing three points where successive Schmidt-hammer impacts were made. Note Schmidt hammer for scale.

Figure 4. Mean Schmidt hammer R-values for successive impacts on the weathered surfaces of nine rock types. A representative 95% confidence interval is shown (all confidence intervals are given in Table 1).

Figure 5. Replication of mean Schmidt hammer R-values for successive impacts on the weathered surfaces of four rock types (representative 95% confidence intervals are shown).

Figure 6. Mean Schmidt hammer R-values (± 95% confidence intervals) for successive impacts on selected unweathered rock surfaces.